

Crystal structures of high temperature quantum paraelectrics $\text{Na}_{1/2}\text{Nd}_{1/2}\text{TiO}_3$ and $\text{Na}_{1/2}\text{Pr}_{1/2}\text{TiO}_3$

This article has been downloaded from IOPscience. Please scroll down to see the full text article.

2006 J. Phys.: Condens. Matter 18 L515

(<http://iopscience.iop.org/0953-8984/18/41/L02>)

View [the table of contents for this issue](#), or go to the [journal homepage](#) for more

Download details:

IP Address: 129.252.86.83

The article was downloaded on 28/05/2010 at 14:23

Please note that [terms and conditions apply](#).

LETTER TO THE EDITOR

Crystal structures of high temperature quantum paraelectrics $\text{Na}_{1/2}\text{Nd}_{1/2}\text{TiO}_3$ and $\text{Na}_{1/2}\text{Pr}_{1/2}\text{TiO}_3$

Rajeev Ranjan^{1,2}, Anupriya Agrawal³, Anatoliy Senyshyn^{4,5} and Hans Boysen¹

¹ Department für Geo- und Umweltwissenschaften, Sektion Kristallographie, Ludwig Mümilian Universität München, Am Coulombwall 1, 85748 Garching, München, Germany

² School of Materials Science and Technology, Institute of Technology, Banaras Hindu University, Varanasi-221005, India

³ Department of Ceramic Engineering, Institute of Technology, Banaras Hindu University, Varanasi-221005, India

⁴ Institute for Materials Science, Darmstadt University of Technology, Petersenstrasse 23, D-64287 Darmstadt, Germany

⁵ Forschungsneutronenquelle Heinz Maier-Leibnitz (FRM II), Technical University München, 85748, Garching, Germany

E-mail: Rajeev.Ranjan@physik.uni-muenchen.de and rranjan@bhu.ac.in

Received 31 May 2006, in final form 27 August 2006

Published 29 September 2006

Online at stacks.iop.org/JPhysCM/18/L515

Abstract

Both neutron and x-ray powder diffraction studies have been carried out for two high temperature quantum paraelectrics, $\text{Na}_{1/2}\text{Nd}_{1/2}\text{TiO}_3$ and $\text{Na}_{1/2}\text{Pr}_{1/2}\text{TiO}_3$. Although visual inspection of the diffraction patterns suggests a ‘nearly cubic’ like structure, careful analysis of powder neutron diffraction patterns and comparison of Rietveld refinement results for competing models reveal that both compounds belong to the orthorhombically distorted GdFeO_3 type of structure ($Pbnm$ space group, $a^-a^-c^+$ tilt system in Glazer notation). The full set of refined structural parameters is reported for the first time. The relationship between octahedral tilt angles and dielectric softness of these compounds is briefly discussed.

1. Introduction

A few members of the perovskite family exhibit the peculiar phenomenon of quantum paraelectricity. The term ‘quantum paraelectric’ was first coined by Muller and Burkard [1] to explain the temperature independent permittivity of SrTiO_3 (ST) below 4 K. The zero point quantum fluctuations preclude stabilization of a ferroelectric state and, as a result, the system remains paraelectric down to the lowest temperature. ST is also known as an incipient ferroelectric [2] at low temperatures. The quantum fluctuations can be suppressed and a ferroelectric state can be induced in ST on the application of an external electric field [3],

pressure [4] or chemical substitution [5, 6]. Subsequently, temperature independence of dielectric permittivity below 50 K has been reported for CaTiO_3 (CT) [7] and for a series of complex perovskites $\text{Na}_{1/2}\text{Ln}_{1/2}\text{TiO}_3$ with $\text{Ln} = \text{Pr, Nd, Sm-Lu}$ [8, 9]. Because of the comparatively high saturation temperatures (T_a), these compounds have been termed ‘high temperature quantum paraelectrics’ [8, 9]. If the origin of the quantum paraelectric behaviour in these high temperature quantum paraelectrics is similar to that proposed by Muller and Burkard for ST, one would also expect a ferroelectric state to stabilize in these systems on suppression of the fluctuations. However, so far no such evidence has been reported in the literature. On the contrary, Ranjan *et al* [10–12], and Chandra *et al* [13] have shown that an intermediate antiferroelectric phase becomes stabilized when CT is substituted by ST, and PbTiO_3 , respectively. This has led to the speculation that CT and the other high temperature quantum paraelectrics might be ‘incipient antiferroelectrics’. More work, however, is needed to understand the nature of incipience of these high temperature quantum paraelectric materials. Raman and infrared reflectivity measurements can be helpful in the search for soft modes responsible for the incipient nature of these compounds. Since crystal structure plays a significant role in determining the dielectric behaviour of perovskites, it is therefore important to have the correct crystal structure information about these compounds. The crystal structures and the phase transition behaviour of ST and CT are well documented in the literature. However, neither detailed structural work nor the phase transition behaviour of most of the other high temperature quantum paraelectrics have been reported so far. In this letter, we present the results of crystal structure studies carried out on two high temperature quantum paraelectric compounds, $\text{Na}_{1/2}\text{Nd}_{1/2}\text{TiO}_3$ (NNT) and $\text{Na}_{1/2}\text{Pr}_{1/2}\text{TiO}_3$ (NPT), using neutron powder diffraction.

2. Experimental details

NNT and NPT were synthesized by a conventional solid state reaction method. Powders of Na_2CO_3 , Nd_2O_3 , Pr_6O_{11} , and TiO_2 , each of purity higher than 99.5%, were thoroughly mixed in stoichiometric ratio in a ball mill with zirconia jars and zirconia balls. Acetone was used as a mixing medium. The mixed powders were calcined at 1000 °C for 3 h and were cold compacted before sintering at 1300 °C in air for 3 h. Sintered pellets were crushed to a fine powder and annealed at 800 °C for ~12 h to remove strains, possibly induced during the crushing process. The sintered powders were checked for their phase purity using a 18 kW Rigaku rotating anode powder diffractometer with copper target and a graphite monochromator in the diffracted beam. Neutron powder diffraction data were collected at the structure powder diffractometer SPODI at the FRM-II research reactor (Garching, Germany) [14] using a wavelength of 1.548 Å.

3. Results and discussion

Figure 1 shows the powder XRD pattern of sintered NNT. All the lines appear as singlets, indicating very weak distortion of the subcell from cubic symmetry. The 111 and 200 pseudocubic reflections are depicted in the inset of this figure. Identical features were noted in the XRD patterns of NPT as well. The Bragg peaks in figure 1 are indexed with respect to a doubled pseudocubic cell $2a_p \times 2b_p \times 2c_p$. Reflections with all-even indices correspond to the pseudocubic subcell. Superlattice reflections have at least one of the indices as an odd integer (e.g., 311, 223 and 214 in figure 1). In general, the superlattice reflections with odd–odd–odd (ooo) and odd–odd–even (ooe) type indices indicate the presence of anti-phase (–) and in-phase (+) tilted octahedra, respectively [15, 16]. These tilts arise due to freezing of soft R_{25} and M_3 phonons of the cubic (space group $Pm\bar{3}m$) phase. In a previous study of

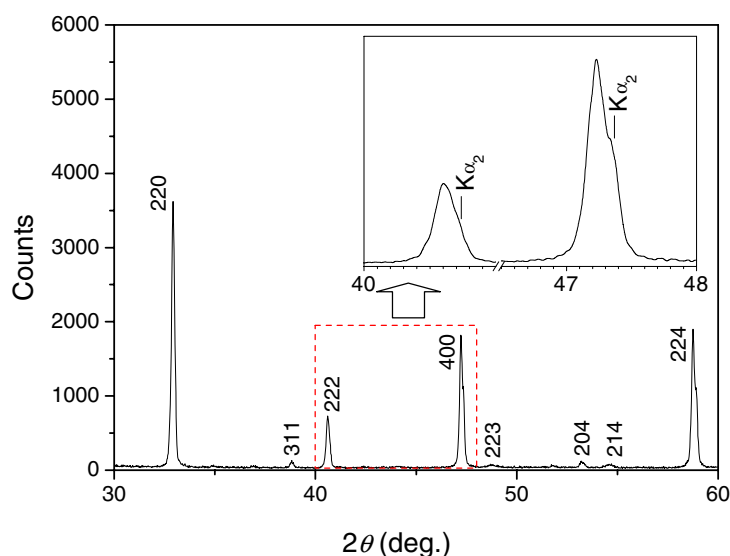


Figure 1. X-ray powder diffraction pattern of $\text{Na}_{1/2}\text{Nd}_{1/2}\text{TiO}_3$ (NNT). The inset shows a magnified view of two Bragg reflections. The asymmetry on the right side of the peaks is due to the $\text{K}\alpha_2$ component in the XRD beam. The indices of the Bragg peaks are shown in accordance with a doubled pseudo-cubic subcell setting.

(This figure is in colour only in the electronic version)

NNT and NPT, Sun *et al* [8] observed ooo(-tilt) and oee type superlattice reflections only using XRD. Belous *et al* [17] have reported a cubic structure for NNT with $a = 3.844(2)$ Å. Since the distortion of the subcell from cubic symmetry is very weak, it is not possible to specify a unique space group merely on the basis of the superlattice reflections observed in powder x-ray diffraction patterns. It may, however, be possible to identify the correct space group by comparing competing models through Rietveld refinement using neutron diffraction data.

Figure 2 depicts the neutron powder diffraction patterns of NNT and NPT in a limited angular 2θ range. Similar to the XRD patterns (figure 1), all the Bragg profiles appear as singlets. The peaks are indexed with respect to a doubled pseudocubic cell ($2a_p \times 2b_p \times 2c_p$). A notable feature of the powder neutron diffraction patterns, missing in the XRD pattern (figure 1), is clear evidence of ooe type superlattice reflection (e.g. 312) characteristic of a '+' tilt. A perusal of the various tilt system given by Glazer [15, 16] suggests that there are four possible space groups: one in the monoclinic system ($P2_1/m$) and three in the orthorhombic system ($Pmmm$, $Pbnm$ and $Cmcm$) which can account for a combination of '+' and '-' tilts. Because of weak distortion of the subcell, only the orthorhombic space groups were considered. Moreover, since the intensities of the superlattice reflections corresponding to the '+' tilt are comparatively weaker than those corresponding to the '-' tilt, the space group $Pmmm$, corresponding to a combination of two '+' and one '-' (i.e. ++-), is less likely. We therefore considered the only two remaining space groups, namely $Cmcm$ and $Pbnm$.

Rietveld refinement was carried out using the software package Fullprof [18]. The pseudo-Voigt function was chosen to model the peak profile shape. The background contribution was determined using a linear interpolation between selected data points in non-overlapping regions. The scale factor, zero angular shift, profile shape parameters, half width (Caglioti) parameters, asymmetry and lattice parameters as well as fractional coordinates of atoms and their displacement parameters were varied during the fitting. Finally, the occupancy

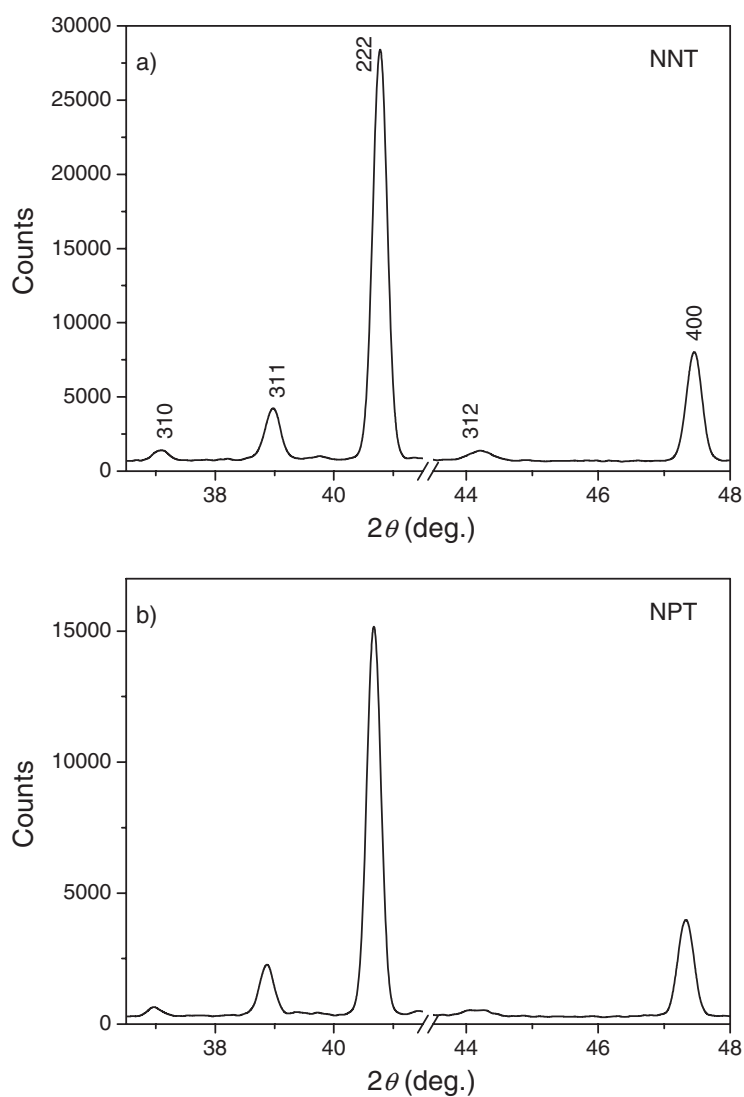


Figure 2. Neutron powder diffraction patterns of (a) $\text{Na}_{1/2}\text{Nd}_{1/2}\text{TiO}_3$ (NNT) and (b) $\text{Na}_{1/2}\text{Pr}_{1/2}\text{TiO}_3$ (NPT) in the 2θ range 36.6° – 48° .

parameters were allowed to vary, but they remained almost close to the nominal composition values within their respective estimated standard deviations (e.s.ds). Initially, refinement with $Pbnm$ and $Cmcm$ structure models was carried out for both NNT and NPT using isotropic displacement parameters only. The goodness of fit was obtained as $\chi^2_{Cmcm} = 4.93$ and $\chi^2_{Pbnm} = 3.51$ for NNT, and $\chi^2_{Cmcm} = 3.07$ and $\chi^2_{Pbnm} = 2.50$ for NPT. Although the difference in χ^2 for NPT is not significantly larger than for NNT, an unusual difference in the isotropic displacement parameter for oxygen in 8e and 8f sites was observed when refined in the $Cmcm$ space group. On the other hand, all the isotropic displacement parameters were well behaved for both compounds when refined in the $Pbnm$ space group. Having identified $Pbnm$ as the correct space group, we refined the anisotropic thermal parameters

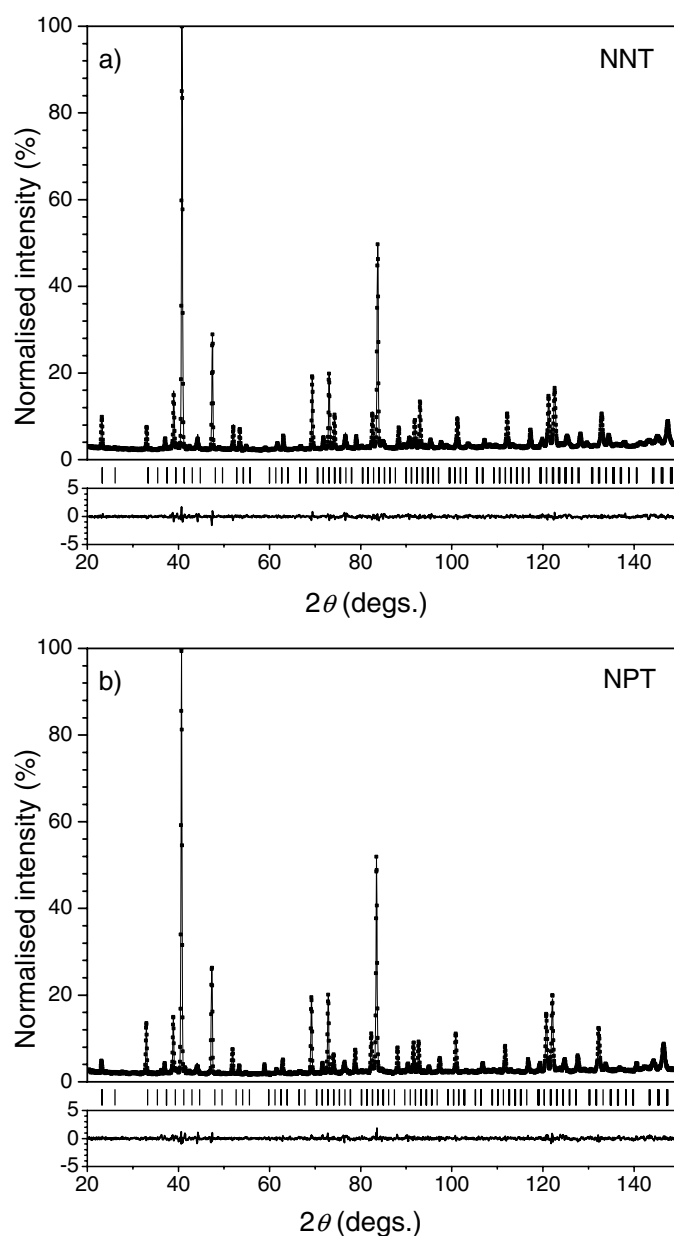


Figure 3. Observed (open circles), calculated (continuous line) and difference (continuous line near the bottom) plots after the final refined cycle in the *Pbnm* space group. The vertical bars indicate positions of the Bragg peaks. (a) $\text{Na}_{1/2}\text{Nd}_{1/2}\text{TiO}_3$ (NNT) and (b) $\text{Na}_{1/2}\text{Pr}_{1/2}\text{TiO}_3$ (NPT).

along with the other structural parameters. This led to a further decrease in the χ^2 values. Figure 3 shows the Rietveld plot of NNT and NPT after the final cycle of refinement with the *Pbnm* space group using anisotropic thermal parameters. An excellent fit with a nearly flat difference plot confirms the correctness of the chosen structural model. The refined structural parameters for both compounds are given in table 1. The subcell lengths

Table 1. Refined structural parameters of NNT and NPT in the $Pbnm$ space group.

		$\text{Na}_{1/2}\text{Pr}_{1/2}\text{TiO}_3$			$\text{Na}_{1/2}\text{Nd}_{1/2}\text{TiO}_3$		
a, b, c (Å)		5.4543(3)	5.4567(1)	7.7085(3)	5.4372(2)	5.4448(2)	7.6930(2)
Na/Pr (Na/Nd)	x, y, z	0.000(2)	0.5121(7)	1/4	0.014(3)	0.506(1)	1/4
	$\beta_{11}/\beta_{22}/\beta_{33}$	0.001(3)	0.007(2)	0.005(1)	0.005(2)	0.005(1)	0.0023(1)
	$\beta_{12}/\beta_{13}/\beta_{23}$	0.001(1)	0	0	0.0012(7)	0	0
Ti	x, y, z	0	0	0	0	0	0
	$\beta_{11}/\beta_{22}/\beta_{33}$	0.000(3)	0.001(1)	0.011(6)	0.000(2)	0.001(2)	0.003(1)
	$\beta_{12}/\beta_{13}/\beta_{23}$	0.006(2)	0.005(2)	0.003(1)	0.005(2)	-0.008(3)	-0.0005(9)
O1	x, y, z	-0.0603(9)	-0.0077(8)	1/4	-0.0561(8)	-0.003(1)	1/4
	$\beta_{11}/\beta_{22}/\beta_{33}$	0.003(2)	0.013(2)	0.0010(8)	0.006(1)	0.011(2)	0.0002(7)
	$\beta_{12}/\beta_{13}/\beta_{23}$	0.002(1)	0	0	0.0003(9)	0	0
O2	x, y, z	0.2252(5)	0.2756(4)	0.0313(5)	0.2318(8)	0.2711(5)	0.0284(5)
	$\beta_{11}/\beta_{22}/\beta_{33}$	0.016(1)	0.001(1)	0.0055(6)	0.0077(8)	0.0024(6)	0.0047(5)
	$\beta_{12}/\beta_{13}/\beta_{23}$	-0.0083(8)	-0.0015(7)	-0.0017(5)	-0.0069(7)	0.0009(5)	-0.0022(5)
R_p, R_{wp}, χ^2 (%)		4.32	5.85	1.90	3.34	4.38	2.26

(a_p, b_p, c_p) obtained from the refined orthorhombic lattice parameters (a_o, b_o, c_o) using the relation $a_p = a_o/\sqrt{2}$, $b_p = b_o/\sqrt{2}$, and $c_p = c_o/2$ are 3.845 Å, 3.850 Å, 3.847 Å, respectively, for NNT and 3.857 Å, 3.859 Å, 3.854 Å, respectively, for NPT. It is therefore evident that the subcell is nearly cubic ($a_p \approx b_p \approx c_p$) in both cases. The cubic lattice parameter ($a = 3.844$ Å) reported by Belous *et al* [17] for NNT is nearly the same as that obtained above. In fact, if one misses the weak superlattice reflections, the diffraction patterns mimic a cubic perovskite structure. Octahedral tilt angles were obtained from the displacements of the O₂ atoms from (0.25, 0.25, 0) to (0.25 - u , 0.25 + v , w). The magnitude of the in-phase tilt (ψ) and the anti-phase tilt (φ), calculated using the expressions $\tan \psi = 2(u + v)$ and $\tan \varphi = 4\sqrt{2}w$ [19], are 5.8° and 10.0°, respectively, for NPT and 4.5° and 9.1°, respectively, for NNT.

First-principles calculations of titanates have shown that hybridization of Ti 3d and O 2p states is essential for ferroelectric distortion to occur [20]. A ‘special’ electronic configuration of the valence orbitals of A site cations in promoting ferroelectric distortion has also been recognized recently [20–22]. For example, the strong covalent character of the Pb–O bond favours a large ferroelastic strain and helps in stabilization of the tetragonal ferroelectric phase in PbTiO₃. First-principles studies of SrTiO₃ and CaTiO₃ have also predicted instability with respect to a zone centre (Γ -point) ferroelectric distortion. However, it is experimentally known that the ground states of these compounds are not ferroelectric but quantum paraelectric. This discrepancy has been qualitatively explained, within the first-principles scheme, in terms of intervention of an instability induced by a non-ferroelectric zone boundary phonon. That is, an antiferrodistortive transition intervenes before the Γ point instability has a chance to freeze in [23]. The tilted octahedra, observed in many of the perovskite compounds, results from freezing of phonons at the M and R points of the Brillouin zone. The fact that the dielectric permittivity of ST, CT and $\text{Na}_{1/2}\text{Ln}_{1/2}\text{TiO}_3$ continues to rise on cooling suggests that the soft nature of the original Γ phonon is preserved even in the tilted octahedral framework.

Figure 4 shows the variation of tilt angle with average value of the A-site cation radius of ($\text{Na}_{1/2}\text{Ln}_{1/2}$)TiO₃. The tilt angles for the compounds other than NPT and NNT were determined using the coordinates of O2 given in [8, 9, 24]. The monotonic increase of the tilt angles with decreasing size of the A-site cation is expected based on consideration of the tolerance factor. An interesting correlation is found between the temperature dependence of

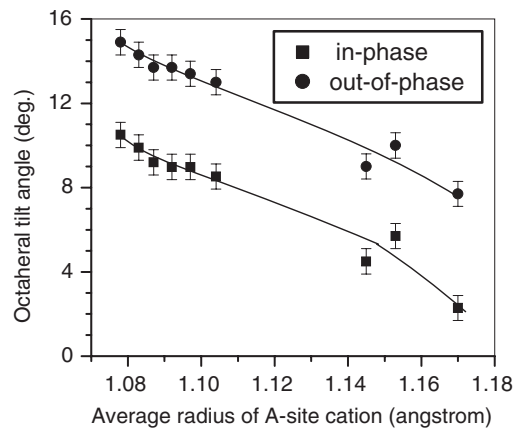


Figure 4. Variation of octahedral in-phase and out-of-phase tilt angles with average radius of the A-site cations in $\text{Na}_{1/2}\text{Ln}_{1/2}\text{TiO}_3$.

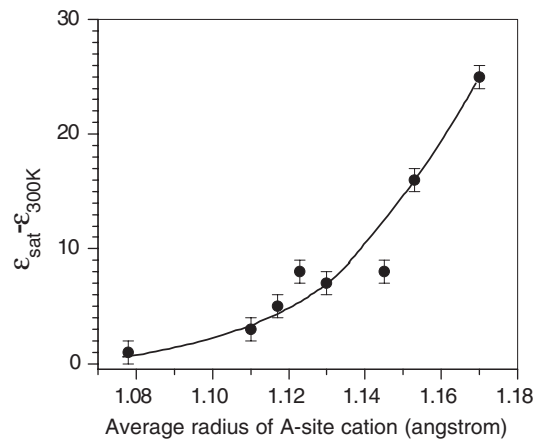


Figure 5. Variation of the difference in dielectric permittivity below the dielectric saturation temperature and 300 K with average radius of A-site cations in $(\text{Na}_{1/2}\text{Ln}_{1/2})\text{TiO}_3$.

polarizability and the average size of the A-site cations in $(\text{Na}_{1/2}\text{Ln}_{1/2})\text{TiO}_3$. Figure 5 shows the difference in the dielectric permittivity of $(\text{Na}_{1/2}\text{Ln}_{1/2})\text{TiO}_3$ below their respective saturation temperature (T_a) and 300 K as a function of average radius of the A-site cation using the data given in [8, 9]. It is evident from this figure that systems with large octahedral tilt exhibit a weak temperature dependence of polarizability. In the lattice dynamical framework, since the temperature dependence of the dielectric permittivity is related to softening of a zone centre phonon, we may conclude that octahedral tilts reduce the softening tendency of the zone centre soft ferroelectric mode. The only way to bring about a ferroelectric phase in tetragonal/orthorhombic/monoclinic perovskites with tilted octahedra will, therefore, depend on the ‘special’ chemistry of the A-site cation.

Rajeev Ranjan is grateful to the Alexander von Humboldt Foundation, Germany, for the award of an AvH fellowship to carry out this work.

References

- [1] Muller K A and Burkard H 1979 *Phys. Rev. B* **19** 3593
- [2] Rytz D, Hochli U T and Bilz H 1980 *Phys. Rev. B* **22** 359
- [3] Hemberger J, Lukenheimer O, Viana R, Bohmer R and Loidl A 1995 *Phys. Rev. B* **52** 13159
- [4] Uwe H and Sakudo T 1976 *Phys. Rev. B* **13** 271
- [5] Bednorz J G and Muller K A 1984 *Phys. Rev. Lett.* **52** 2289
- [6] Lemarov V V, Smirnova E P, Syrnikov P P and Tarakanov E A 1996 *Phys. Rev. B* **54** 3151
- [7] Kim I S, Itoh M and Nakamura T 1992 *J. Solid State Chem.* **101** 77
- [8] Sun P-H, Nakamura T, Shan Y J, Inaguma Y and Itoh M 1997 *Ferroelectrics* **200** 93
- [9] Shan Y J, Nakamura T, Inaguma Y and Itoh M 1998 *Solid State Ion.* **108** 123
- [10] Ranjan R, Pandey D and Lalla N P 2000 *Phys. Rev. Lett.* **84** 3726
- [11] Ranjan R and Pandey D 2001 *J. Phys.: Condens. Matter* **13** 4239
- [12] Ranjan R and Pandey D 2001 *J. Phys.: Condens. Matter* **13** 4251
- [13] Chandra A, Ranjan R, Singh D P, Khare N and Pandey D 2006 *J. Phys.: Condens. Matter* **18** 2977
- [14] Gilles R, Krimmer B, Boysen H and Fuess H 2002 *Appl. Phys. A* **74** S148
- [15] Glazer A M 1972 *Acta Crystallogr. B* **28** 3384
- [16] Glazer A M 1975 *Acta Crystallogr. A* **31** 756
- [17] Belous A, Novitskaya N, Antishko A, Gavrilova L, Polyanetskaya S and Makarova Z 1985 *Sov. Prog. Chem.* **51** 13
- [18] Rodrigues-Carvajal J 2000 FULLPROF. A Rietveld refinement and pattern matching analysis program. Laboratoire Leon Brillouin (CEA-CNRS) France
- [19] Kennedy B J, Howard C J and Chakoumakos B C 1999 *J. Phys.: Condens. Matter* **11** 1479
- [20] Cohen R E 1992 *Nature* **358** 136
- [21] Hill N A 2005 *Annu. Rev. Mater. Res.* **32** 1
- [22] Ederer C and Spaldin N A 2005 *Preprint cond-mat/0512330*
- [23] Zhong W and Vanderbilt D 1995 *Phys. Rev. Lett.* **74** 2587
- [24] Mitchell R H and Chakhmouradian A R 1998 *J. Solid State Chem.* **138** 307